A continuous-wave Nd:YVO_4-KGW intracavity Raman laser with over 34% diode-to-Stokes optical efficiency

Quan Sheng [1,2], Jingni Geng [1,2], Tianchang Liu [1,2], Shijie Fu [1,2,*], Wei Shi [1,2,*], and Jianquan Yao [1,2]

[1] *Institute of Laser and Optoelectronics, School of Precision Instrument and Optoelectronics Engineering, Tianjin University, Tianjin 300072, China*

[2] *Key Laboratory of Optoelectronic Information Technology (Ministry of Education), Tianjin University, Tianjin 300072, China*

Abstract We demonstrate a continuous-wave (CW) Nd:YVO_4-KGW intracavity Raman laser with a diode-to-Stokes optical efficiency of 34.2%. By optimizing the cavity arrangement and reducing the cavity losses, 8.47 W Stokes output at 1177 nm was obtained under an incident 878.6 nm diode pump power of 24.8 W. The influence of cavity losses on the power and efficiency of the CW Raman laser, as well as the potential for further optimization, were investigated based on the numerical model. The observation of thermal-induced output rollover was well explained by the calculation of the thermal lensing and cavity stability, indicating that the end-face curvature played an important role when the end-face of the crystal is highly-reflective coated to make the cavity. 10.9 W Stokes output under 40.9 W incident pump was also demonstrated with cavity arrangement less sensitive

This peer-reviewed article has been accepted for publication but not yet copyedited or typeset, and so may be subject to change during the production process. The article is considered published and may be cited using its DOI.

10.1017/hpl.2024.5

to the end-face curvature, which is the highest output power of CW intracavity Raman lasers reported.

*Correspondence to: Shijie Fu, and Wei Shi, School of Precision Instrument and Optoelectronics Engineering, Tianjin University, Tianjin 300072, China. E-mail: shijie_fu@tju.edu.cn; shiwei@tju.edu.cn

Key words: *intracavity Raman laser, continuous-wave, KGW crystal, thermal lens*

I. INTRODUCTION

Solid-state Raman lasers based on stimulated Raman scattering (SRS) in crystalline Raman gain media have been established as reliable laser sources for wavelength regions difficult to be obtained directly with population inversion lasers [1,2]. Benefiting from the automatic phase matching and beam clean-up characteristics of the SRS process, the Raman lasers can generate output in the whole transparent range of the gain media with good beam quality. Combined with second harmonic generation (SHG) and/or sum-frequency generation (SFG) technique, Raman lasers with output from ultraviolet to mid-infrared have been demonstrated with various Raman crystals including tungstate, vanadate, nitrate, niobate, as well as recently developed diamond which benefits very high Raman gain coefficient, damage threshold, and thermal conductivity [3-8].

As a third-order nonlinear process, the SRS gain relies on the high fundamental laser intensity significantly. For continuous-wave (CW) Raman lasers, tens of watts fundamental laser power are usually required to reach the SRS threshold [8], despite the tightly focused and double-pass pump scheme being utilized. Therefore, the intracavity pump scheme (including the self-Raman scheme) is preferred in low-to-moderate power CW Raman lasers. Incorporating the Raman gain medium inside the fundamental laser cavity to make use of high intracavity powers, efficient CW Raman

https://doi.org/10.1017/hpl.2024.5 Published online by Cambridge University Press

conversion can be realized under watt-level laser diode (LD) pump power [10-12]. Multi-watt CW near-infrared Stokes output and versatile visible harmonic output from intracavity Raman lasers have been demonstrated by several research groups [10-13].

One main issue that limits the power and efficiency scaling of CW Raman lasers is the cavity losses. Most of the CW Raman lasers have the output coupling at the level of 1-2% or lower (including those with high-Q Stokes cavity and intracavity SHG/SFG nonlinear coupling for visible output) because of the low gain. Therefore, even tiny passive Stokes cavity losses would decrease the slope efficiency and increase the threshold of the laser seriously. The fundamental cavity losses would also weaken the coupling from the fundamental field to the Stokes wave. A comprehensive model on the efficiency of CW intracavity Raman lasers has been presented by Spence *et al*. [14,15]. Based on their model, decreasing the round-trip losses of the fundamental and Stokes fields from 1% to 0.5% may increase the optical efficiency of the Raman laser from 18% to 39%. In 2016, Fan *et al*. reported a self-Raman laser based on YVO_4/Nd:YVO_4/YVO_4 crystal. With self-Raman scheme minimizing the insertion losses, they got 5.3 W CW Stokes output at 1176 nm with an optical efficiency of 20% [10]. In 2021, Chen *et al*. demonstrated a frequency-doubled CW Nd:$GdVO_4$-KGW intracavity Raman laser. With a highly reflective (HR) mirror being optimized to decrease the non-unity reflection losses of the fundamental and Stokes waves, the quasi-continuous-wave (QCW) yellow output power was improved significantly from 5.7 W to 10.5 W, with conversion efficiency increased from 15% to 26.3% [13].

Another issue is the strong thermal lensing occurs in both the laser and Raman crystals at high pump levels [13,16]. For example, the yellow Raman laser in [13] could deliver 10.5 W instantaneous QCW output when operating with a 50% pump duty circle to alleviate the thermal load, but the maximum output power in the CW scheme was limited to 4.5 W because of the

https://doi.org/10.1017/hpl.2024.5 Published online by Cambridge University Press

thermal lensing. Therefore, determining the strength of thermal lensing and making corresponding compensation via cavity design is essential for high-power Raman laser output.

In this work, we demonstrate an efficient CW Nd:YVO_4-KGW intracavity Raman laser. To minimize the cavity losses, we used a KGW Raman crystal with HR Stokes coating on one of its end-faces to remove the necessity of a separated dichroic mirror usually used. With this design, the efficiency of the Raman laser was improved a lot compared with that using a separated dichroic mirror to make the Stokes cavity. 8.47 W CW Stokes output at 1177 nm was obtained under an incident LD pump power of 24.8 W, with the optical efficiency being 34.2%, which is the highest efficiency of CW intracavity Raman lasers reported. The influence of cavity losses on the power and efficiency of the Raman laser is analyzed based on the rate equation model. Besides, we found that the influence of thermal lensing on cavity stability differed a lot with the two Stokes cavity arrangements because the thermal-induced end-face curvature played different roles. The detailed calculation on the thermal lensing and cavity stability explained the experimental observation well.

II. EXPERIMENTAL ARRANGEMENT

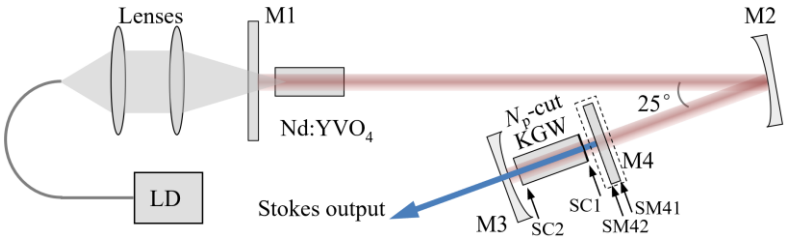

Figure. 1. Experimental setup of the Nd:YVO_4-KGW intracavity Raman laser with Stokes HR coating on one of the crystal end-faces and on a separate mirror.

Figure 1 depicts the experimental arrangement. The pump source was a fiber-coupled wavelength-stabilized LD at 878.6 nm with a maximum power of 65 W, with a fiber core diameter of 400 μm

https://doi.org/10.1017/hpl.2024.5 Published online by Cambridge University Press

and a numerical aperture of 0.22. The pump light was focused onto the input face of an *a*-cut Nd:YVO_4 crystal used as the gain medium of the 1064 nm fundamental laser with a spot radius of 280 μm. The 3×3×15 mm^3 Nd:YVO_4 crystal (CASTECH Inc.) with a doping concentration of 0.2-at.% absorbed ~80% of the incident random polarized pump light. The folded cavity of the 1064 nm fundamental laser was defined by a flat HR mirror M1, a concave HR mirror M2 with a radius of curvature (RoC) of 100 mm, and a concave HR mirror M3 with a RoC of 200 mm. The M3 also served as the Stokes output coupler, with a transmittance of T_S=0.7% at 1177 nm. The distances M1-M2 and M2-M3 were 168 mm and 65 mm, respectively. The folding angle was set as small as possible to be 25° (full angle) to minimize the influence of astigmatism. A 3×3×20 mm^3 KGW crystal cut along its N_p-axis (CASTECH Inc.) was used as the Raman gain medium. The laser and Raman crystals were oriented to have the 1064 nm fundamental laser polarized along the N_m axis of the KGW crystal, to make use of the strong 901 cm^{-1} Raman gain for 1177 nm Stokes output while suppressing the 768 cm^{-1} Raman line and cascaded Raman conversions [17]. The Nd:YVO_4 crystal and KGW crystal were wrapped in indium foil and mounted in aluminum holders water cooled at 20°C, and located close to the mirror M1 and M3, respectively.

In the experiment, we tried two different Stokes cavity arrangements. To minimize the fundamental and Stokes cavity losses L_F and L_S which may limit the laser efficiency seriously, we used a KGW crystal with 1064 nm anti-reflecting (AR) coating on both faces (marked as SC1 and SC2 in Figure 1) and 1177 nm HR coating on one face (SC1), to remove the necessity of an additional dichroic mirror M4 (AR@1064 nm on both of its faces SM41 and SM42, and HR@1177nm on one face SM42, from CRYSTECH Inc.) for Stokes cavity. For comparison, we also used a KGW crystal coated for AR at both 1064 nm and 1177 nm on both faces and the separate dichroic mirror M4 to make the Stokes cavity with the output coupler M3. The Stokes

https://doi.org/10.1017/hpl.2024.5 Published online by Cambridge University Press

cavity lengths were 22 mm for the case with HR coating on crystal and 23 mm when using the separate HR mirror M4. Table 1 gives the reflectivities of the AR coatings and transmittances of the HR coating of each surface provided by the manufacturers, which are different for the two cavity arrangements. The other unchanged elements, including M1, M2, M3 and the Nd:YVO_4 crystal, brought a total round-trip loss of 0.2% to the fundamental laser. For the case with the Stokes HR coating on the crystal end-face SC1, the sum of the unwanted reflectivities and transmittances of the 1064 nm fundamental laser cavity for a round-trip was 1.94%, comparable to that of 1.55% when using the separate HR mirror M4 to make the Stokes cavity. However, the sum of the unwanted reflectivities and transmittances for the Stokes wave in its cavity was reduced significantly from 0.94% to 0.27%. Considering the rather low Stokes output coupling of 0.7%, reducing the Stokes cavity loss may help to enhance the Raman laser efficiency significantly.

Table. 1 The reflectivities of the AR coatings and transmittances of the HR coating of each surface provided by the manufacturers.

Cavity arrangement with HR mirror M4			Cavity arrangement with HR coating on KGW		
Surfaces	1064nm	1177nm	Surfaces	1064nm	1177nm
SC1	R=0.144%	R=0.22%	SC1	R=0.54%	T=0.03%
SC2	R=0.36%	R=0.23%	SC2	R=0.33%	R=0.12%
SM41	R=0.01%	/			
SM42	R=0.16%	T=0.037%			
The sum of the unwanted R and T for a round-trip	1.55%	0.94%	The sum of the unwanted R and T for a round-trip	1.94%	0.27%

III. EXPERIMENTAL RESULTS

https://doi.org/10.1017/hpl.2024.5 Published online by Cambridge University Press

Figure 2 shows the output power of the 1177 nm Stokes wave (P_{S_out}) as a function of the incident LD pump power (P_P), measured using a laser powermeter Ophir VEGA with sensor 30A-BB-18. The 1064 nm leakage power recorded behind the mirror M2 was also plotted in the figure. We can see that with the Stokes cavity losses reduced by removing the separate dichroic mirror M4, the Raman laser with KGW crystal HR coated for Stokes wave exhibited lower SRS threshold and enhanced conversion efficiency (black dot), compared with the case with AR coated crystal and the dichroic mirror. With the same T_S=0.7% Stokes output coupler, the SRS threshold was decreased from 4.3 W to 2.2 W incident LD power. The Stokes output power reached 8.47 W under the incident pump power of 24.8 W, with optical efficiency and slope efficiency being 34.2% and 38.6%, respectively. To the best of our knowledge, this is the first demonstration of CW intracavity Raman laser with optical efficiency over 30%, which is mainly attributed to the cavity design optimized for mode-matching and reduction of cavity losses. Note that the Nd:YVO_4 crystal absorbed only 80% of the incident pump, the conversion efficiency with respect to absorbed pump power reached 42.8%. However, the increase of Stokes output power became quite slow thereafter, and finally rolled over when the pump power exceeded 29.1 W (with Stokes output power of 8.68 W).

https://doi.org/10.1017/hpl.2024.5 Published online by Cambridge University Press

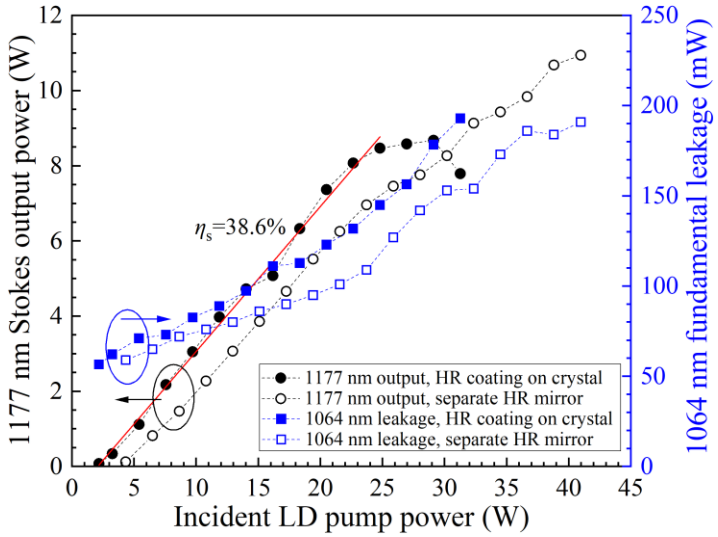

Figure 2. Stokes output power and fundamental laser leakage as a function of incident LD pump power, with the two different cavity arrangements.

For comparison, when using the separate dichroic mirror M4, the Stokes output powers (black empty circle) were much lower than those with the HR-coated KGW under the same pump power below 27 W, due to the higher Stokes cavity losses. Nevertheless, the rollover did not occur with this cavity arrangement even at the maximum pump power used in the experiment of 40.9 W. A maximum Stokes output power of 10.9 W was obtained, with optical efficiency being 26.6%. This is the highest output power of CW crystalline Raman lasers with gain media besides the newly developed diamond crystal, including in both intracavity and extracavity schemes. We did not further increase the pump power considering the risk of components damage given the high circulating power in the cavity.

Figure 3 shows some typical spectra and beam profiles, recorded using an optical spectrum analyzer Yokogawa 6370D (resolution 0.02 nm) and a CCD camera SP907, respectively. The Stokes spectra broadened with the increasing pump power, and were multi-line with linewidths of ~0.3 nm at the maximum pump. Compared with our previous work in which a T_S=0.4% output

https://doi.org/10.1017/hpl.2024.5 Published online by Cambridge University Press

coupler was used [17], neither cascaded Raman lines nor second Stokes lines were observed here, since the higher output coupling of T_S=0.7% decreased the intracavity Stokes power. The Stokes beam profile became elliptic when the output power was over 5 W because of the astigmatic thermal lens in the KGW crystal and finally became multi-lobe high-order Hermite-Gaussian mode [16].

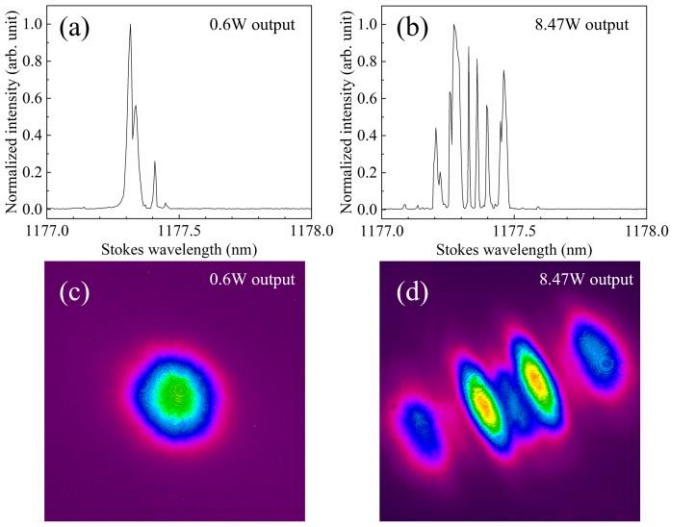

Figure 3. Typical Stokes spectra (a), (b) and beam profiles (c), (d) at different Stokes output powers, with the HR-coated KGW crystal.

IV. DISCUSSION

Stokes power/efficiency and cavity losses

The experimental results showed that the efficiency of the Raman laser was quite sensitive to the cavity losses. The influence of cavity losses on the power/efficiency of the Raman laser is then estimated based on the model presented by Spence *et al*. in ref [15], with backward Raman gain taken into consideration for the CW operation scheme. With the thermal lens in the crystal

https://doi.org/10.1017/hpl.2024.5 Published online by Cambridge University Press

considered, the average TEM_{00} mode beam radii of 1064 nm fundamental laser in the Nd:YVO_4 crystal and the KGW crystal were calculated to be 270 μm and 80 μm, respectively, while the TEM_{00} mode beam radius of the Stokes field in the KGW crystal was 110 μm. Considering the fundamental laser usually operates in multi-transverse-mode when intracavity SRS occurs, the fundamental beam radius at KGW used in the power/efficiency simulation was 110 μm. The Raman gain coefficient of the KGW crystal used in the calculation was 3 cm/GW rather than the steady-state Raman gain coefficient of 4.5 cm/GW for 1064 nm fundamental laser polarized along N_m axis, with the influence of fundamental and Stokes spectral broadening on the effective Raman gain considered [15].

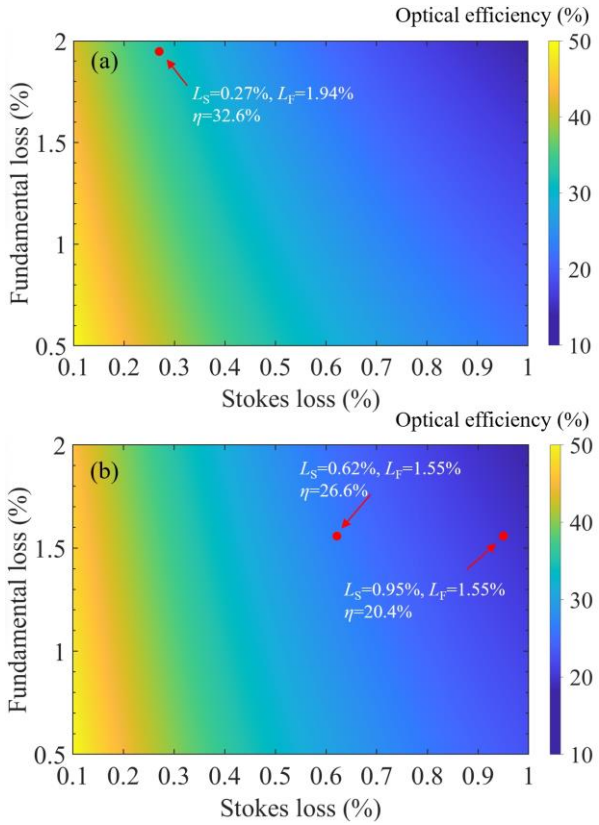

Figure 4. Optical efficiency P_{S_out}/P_P of the Raman laser as a function of the Stokes and fundamental round-trip losses, with the incident pump power of (a) 24.8 W and (b) 40.9W,

https://doi.org/10.1017/hpl.2024.5 Published online by Cambridge University Press

respectively. The calculation used a 270-μm fundamental laser radius in the laser crystal, a 110-μm both of the fundamental laser radius and the Stokes beam radius in the KGW crystal, and a 0.7% output coupling for the Stokes wave.

Figure 4 plots the calculated optical efficiency P_{S_out}/P_P of the intracavity Raman laser as a function of the fundamental and Stokes round-trip losses. As shown in Figure 4(a), for the case using the KGW crystal with HR Stokes coating, the calculated optical efficiency of 32.6% under the pump power of 24.8 W matched very well with the experimental result of 32.4%. From the figure we can see that reducing the Stokes cavity losses is critical for optimizing the laser efficiency, because of the low output coupling. Besides, if round-trip losses of the fundamental laser L_F can be reduced to 0.5% or lower, the optical efficiency of the CW intracavity Raman laser can be further improved to the level of 40-45%. For the separate dichroic mirror cavity arrangement with round-trip losses of L_F=1.55% and L_S=0.94% for fundamental and Stokes, respectively, the calculated optical efficiency was 20.4% under 40.9 W pump (Figure 4(b)), lower than the experimental value of 26.6%. This reveals that the actual round-trip losses may be lower than that calculated by adding up the unwanted reflectivities and transmittances provided by the elements manufacturers in Table 1. For example, in this arrangement with separated dichroic mirror M4, the calculated Stokes losses L_S mainly came from the coatings on the two faces of the KGW crystal with quite similar reflectivities. The actual (single-pass) loss may be lower than the sum of the two due to the weak etalon effect between the two parallel surfaces. Considering the influence of L_F is not as significant as that of the Stokes, the deviation between the calculated and experimental values was mainly due to the overestimated L_S. Assuming an L_F of 1.55%, the L_S should be approximately 0.62% (including the nonnegligible absorption loss induced by the Tm^{3+}

https://doi.org/10.1017/hpl.2024.5 Published online by Cambridge University Press

impurity which caused the strong blue fluorescence [18]) for the experimental optical efficiency of 26.6% under incident pump power of 40.9 W.

The influence of KGW crystal end-face curvature

It was interesting that the maximum Stokes output powers before rollover were quite different with the two cavity arrangements. In fact, we also tried output couplers with transmittances of 0.4% and 1.1% in the experiment. With all these output couplers, the rollover of Stokes output power occurred much earlier when using the HR-coated KGW crystal than that with the separate dichroic mirror M4. We can see from Figure 2 that the 1064 nm leakage behind the folding mirror M2 (blue solid square) kept growing after the rollover of the Stokes output occurred, revealing that the rollover was due to the stability issue of the Stokes cavity, rather than that of the fundamental laser cavity.

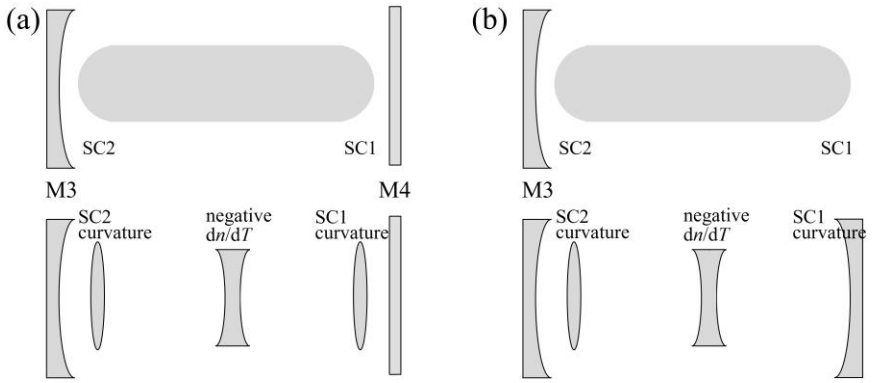

Figure 5. The schematic of the influences of the end-face curvature on the cavity scheme.

The only difference between the two Stokes cavity arrangements is the dichroic mirror M4 used to make the Stokes cavity is replaced by the HR coating on the KGW. In these two arrangements, the influences of thermal-induced end-face curvature of the surface SC1 on the cavity stability are

https://doi.org/10.1017/hpl.2024.5 Published online by Cambridge University Press

different. Different from conventional single-end-pumped inversion lasers, the SRS thermal load in KGW crystal distributed uniformly along the crystal length. As shown in Figure 5(a), the negative thermo-optic coefficient dn/dT of the KGW crystal induced strong negative thermal lensing f_{tn}, which can be seen as a thin lens in the middle of the crystal. By contrast, the end-face curvature due to the thermal-expansion introduced positive thermal lensing f_{te} at both of the two end-faces. In this case, the *ABCD* matrix of SC1-M4-SC1 (go through the end-face SC1 twice) is [1, 0; $-2/f_{te}$, 1], when neglecting the small distance of ~1 mm between the crystal and the mirror M4. The f_{te} here is the thermal lens focal length of the *single* curved end-face induced by thermal expansion. For the case with HR Stokes coating on KGW crystal, as shown in Figure 5(b), the SC1-M4-SC1 is replaced by a concave reflecting surface SC1 with *ABCD* matrix of [1, 0; $-1/(R_e/2)$, 1], where R_e is the thermal-expansion-induced RoC of the end-face SC1, with its relationship between f_{te} being $R_e = 2f_{te}(n-1)$ [19], where n is the refractive index of the crystal (n=1.99 for 1177 nm Stokes polarized along N_m axis of the KGW crystal). For the KGW crystal with large negative dn/dT, it is the strong negative thermal lensing makes the Stokes cavity unstable, while the positive end-face curvature would compensate the negative thermal lensing to some extent [20]. When using the separate dichroic mirror M4 to make the Stokes cavity with output coupler M3, the oscillating beam passed through the focusing surface SC1 twice, therefore experiencing stronger positive thermal lensing compared with the case using HR coated KGW crystal, so that compensated the negative thermal lensing more and allowed the laser to operate with higher Stokes power.

The thermal lens focal length induced by the thermo-optic coefficient and end-face curvature of the Raman crystal KGW can be estimated using the following equations [19,20],

https://doi.org/10.1017/hpl.2024.5 Published online by Cambridge University Press

$$f_{\mathrm{tn}}=\frac{k_C\pi w_S^2}{P_{\mathrm{h}}}\left(\frac{\mathrm{d}n}{\mathrm{d}T}\right)^{-1} \tag{1}$$

$$f_{\mathrm{te}}=\frac{k_C\pi w_S^2}{P_{\mathrm{h}}}\left(\frac{\alpha r_0(n-1)}{l}\right)^{-1} \tag{2}$$

where k_C is the thermal conductivity, w_S is the Stokes beam radius, α is the thermal expansion coefficient, r_0 is the radius of the crystal end-face, l is the crystal length, $P_h=P_S(\lambda_S/\lambda_L-1)$ is the heat generated, λ_S and λ_L in which are Stokes and fundamental wavelengths, respectively. Note that the P_S in the equations is Stokes power generated rather than the output power from the output coupler P_{S_out}, with the relationship $P_{S\_out}=P_S\times T_S/(T_S+L_S)$. For the Stokes cavities with HR coated KGW crystal and separated dichroic mirror M4 here, P_S are 1.39 and 1.89 times of P_{S_out}, respectively. For the N_p-cut KGW crystal with laser polarized along its N_m axis, we have $\mathrm{d}n/\mathrm{d}T=-0.8\times10^{-6}$ K^{-1}, k_C=3.4 W/(m·K) and $\alpha=1.6\times10^{-6}$ K^{-1} [21].

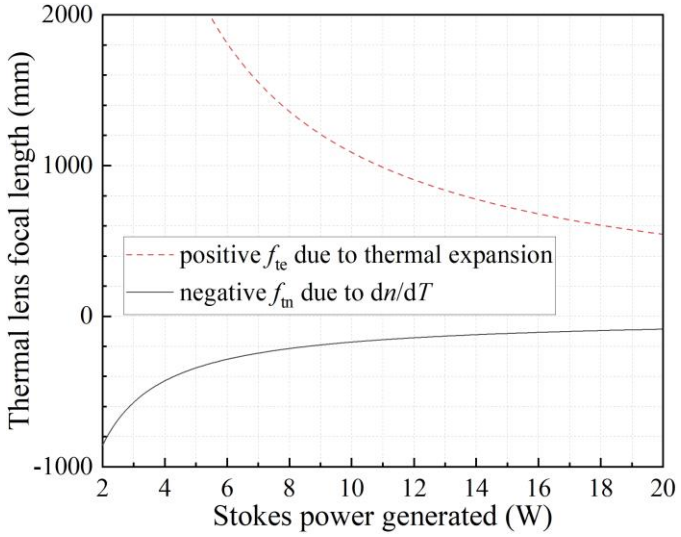

Figure 6. Thermal-optic induced negative thermal lens focal length and (single) end-face curvature induced positive thermal lens focal length as a function of Stokes power generated in KGW crystal,

https://doi.org/10.1017/hpl.2024.5 Published online by Cambridge University Press

in p[mm]p orientation. The fundamental and Stokes wavelengths are 1064 nm and 1177 nm, respectively. The Stokes beam radius in KGW crystal used in calculation is 110 μm.

Figure 6 plots calculated negative f_{tn} and the positive f_{te} as a function of the generated Stokes power. Both of them became stronger with the increasing Stokes power. The f_{tn} are -343 mm, -171.5 mm, and -114.4 mm, respectively, with 5 W, 10 W, and 15 W Stokes power generated, while the f_{te} are 2174 mm, 1087 mm, and 725 mm. The gradient of the lens strength with respect to the generated Stokes power are 0.58 D/W and 0.092 D/W, respectively. With the relationship between f_{tn} and f_{te} determined, we can further calculate their influence on the cavity stability with the two different Stokes cavity arrangements depicted in Figure 5, as shown in Figure 7. With the HR-coated KGW crystal, the cavity would become unstable with the negative f_{tn} shorter than -155 mm, while the f_{te} is 972 mm. For the Stokes cavity with separate dichroic mirror M4, the positive f_{te} compensates more on the negative f_{tn}, and the cavity allows the f_{tn} as short as -135 mm (with the corresponding f_{te} being 856 mm). The calculation results could well explain why the rollover of Stokes power occurred earlier when using the HR-coated KGW crystal than with the separate M4, despite the contribution of photoelastic effect is neglected in the calculation. Moreover, the fundamental mode beam size of the Stokes wave would expand significantly before the cavity became unstable. The astigmatic thermal lensing in the KGW crystal also makes the Stokes field operate in high-order transverse mode [16]. These issues may weaken the thermal lensing to some extent. Considering the current limitation of Stokes cavity stability on output power with the HR-coated KGW crystal, one can use output coupler M3 with a smaller RoC that allows stronger negative thermal lensing for higher power.

https://doi.org/10.1017/hpl.2024.5 Published online by Cambridge University Press

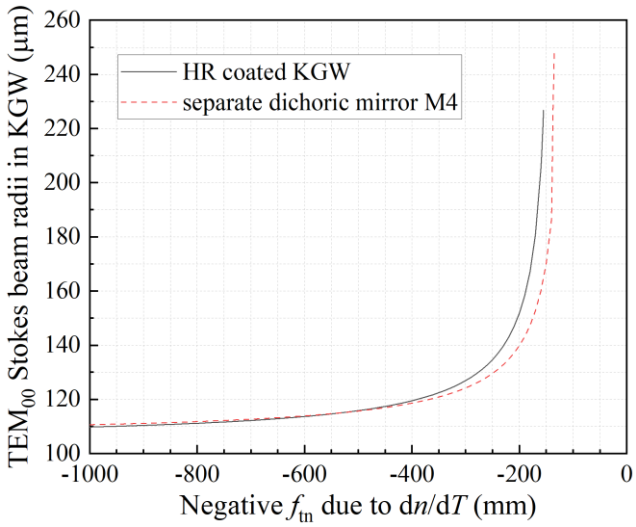

Figure 7. TEM_{00} mode Stokes beam size evolution with thermal-optic induced f_{tn} in KGW crystal with the two different cavity arrangements, with the relationship between f_{tn} and f_{te} considered.

From Figure 4 we know that the optical efficiency of the CW intracavity Raman laser could reach 40% or higher with proper control of cavity losses and output coupling. The KGW crystal is capable of generating tens of watts output with very good beam quality when serving as the host of inversion laser gain media, with cavity design well compensates the strong astigmatic thermal lensing [22]. Therefore, we can expect 20-30 W CW output from such end-pumped intracavity Raman lasers with conventional Raman crystals like KGW. It should be mentioned that this level of output power is still 1-2 orders of magnitude lower than those of the state-of-the-art extracavity diamond Raman lasers, with which 154 W CW output and 1.2 kW QCW peak power have been demonstrated by virtue of the superior thermal properties and Raman gain of the diamond crystal [23,24]. However, the intracavity approaches with cheap and easily accessible conventional Raman crystals still provide a very efficient and low-threshold choice for versatile output wavelengths with 10-W or higher power under low-to-moderate primary pump power.

V. CONCLUSION

https://doi.org/10.1017/hpl.2024.5 Published online by Cambridge University Press

In conclusion, we have demonstrated an efficient CW Nd:YVO_4-KGW intracavity Raman laser. By using Raman crystal with one of its end-faces coated for HR at Stokes length to remove the dichroic mirror and reduce the cavity losses, 8.47 W Stokes output at 1177 nm was obtained under the incident pump power of 24.8 W, with optical efficiency being 34.2%, which is the highest among CW intracavity Raman lasers reported. The influence of cavity losses on the power and efficiency of the Raman laser was investigated based on the numerical model. Besides, it was observed that the output rollover related to thermal lensing is quite different for Stokes cavities with HR coated crystal end-face and with dichroic mirror as the total reflector. The calculation on the thermal lensing and cavity mode revealed that the thermal-induced end-face curvature of KGW crystal has different effects on the cavity stability with the two cavity arrangements.

Acknowledgment

This work was supported by the National Natural Science Foundation of China (61975146, 62105240, 62075159, and 62275190); Shandong Province Key R&D Program (2020CXGC010104, 2021CXGC010202); Seed Foundation of Tianjin University (2023XPD-0020).

References

1. Casula, R., Penttinen, J., Guina, M., Kemp, A. J., and Hastie, J. E., "Cascaded crystalline Raman lasers for extended wavelength coverage: continuous-wave, third-Stokes operation," Optica 5(11), 1406-1413 (2018).
2. Pask, H. M., Dekker, P., Mildren, R. P., Spence, D. J., and Piper, J. A., "Wavelength-versatile visible and UV sources based on crystalline Raman lasers," Prog. Quantum. Electron. 32(3-4), 121-58 (2008).
3. Gelbach, N., Neustadter, Y., Henig, M., Nahear, R., and Noach, S., "Two-mJ level, high-energy all-passive KGW/Tm:YLF Raman laser," Opt. Lett. 48(17), 4444-4447 (2023).

https://doi.org/10.1017/hpl.2024.5 Published online by Cambridge University Press

4. Sheng, Q., Lee, A. J., Spence, D. J., and Pask, H. M., "Wavelength tuning and power enhancement of an intracavity Nd:$GdVO_4$-$BaWO_4$ Raman laser using an etalon," Opt. Express 26(24), 32145-32155 (2018).
5. Duan, Y., Sun, Y., Zhu, H., Mao, T., Zhang, L., and Chen, X., "YVO_4 cascaded Raman laser for five-visible-wavelength switchable emission," Opt. Lett. 45(9), 2564-2567 (2020).
6. Zhao, H., Lin, C., Jiang, C., Dai, S., Zhou, H., Zhu, S., Yin, H., Li, Z., and Chen, Z., "Wavelength-versatile deep-red laser source by intracavity frequency converted Raman laser," Opt. Express 31(1), 265-273 (2023).
7. Warrier, A. M., Lin, J., Pask, H. M., Lee, A. J., and Spence, D. J., "Multiwavelength ultrafast $LiNbO_3$ Raman laser," Opt. Express 23(20), 25582-25587 (2015).
8. Bai, Z., Williams, R. J., Kitzler, O., Sarang, S., Spence, D. J., and Mildren, R. P., "302 W quasi-continuous cascaded diamond Raman laser at 1.5 microns with large brightness enhancement," Opt. Express 26(16), 19797-19803 (2018).
9. Liu, Y., Zhu, C., Sun, Y., Mildren, R., Bai, Z., Zhang, B., and Feng, Y., "High-power free-running single-longitudinal-mode diamond Raman laser enabled by suppressing parasitic stimulated Brillouin scattering,". High Power Laser Sci. Eng. 11, e72 (2023).
10. Fan, L., Zhao, W., Qiao, X., Xia, C., Wang, L., Fan, H., and Shen, M., "An efficient continuous-wave YVO_4/Nd:YVO_4/YVO_4 self-Raman, laser pumped by a wavelength-locked 878.9 nm laser diode," Chin. Phys. B 25(11), 114207 (2016).
11. Sheng, Q., Li, R., Lee, A. J., Spence, D. J., and Pask, H. M., "A single-frequency intracavity Raman laser," Opt. Express 27(6), 8540–8553 (2019).
12. Liu, Y. C., Chen, C. M., Hsiao, J. Q., Pan, Y. Y., Tsou, C. H., Liang, H. C., and Chen, Y. F., "Compact efficient high-power triple-color Nd:YVO_4 yellow-lime-green self-Raman lasers," Opt. Lett. 45(5), 1144-1147 (2020).
13. Chen, Y. F., Li, D., Lee, Y. M., Lee, C. C., Huang, H. Y., Tsou, C. H., and Liang, H. C., "Highly efficient solid-state Raman yellow-orange lasers created by enhancing the cavity reflectivity," Opt. Lett. 46(4), 797-800 (2021).
14. Spence, D. J., Dekker, P., and Pask, H. M., "Modeling of continuous wave intracavity Raman lasers," IEEE J. Sel. Topics Quantum Electron. 13(3), 756-763 (2007).

https://doi.org/10.1017/hpl.2024.5 Published online by Cambridge University Press

15. Spence, D. J., “Spatial and spectral effects in continuous-wave intracavity Raman lasers,” IEEE J. Sel. Topics Quantum Electron. 21(1), 1400108 (2015).
16. McKay, A., Kitzler, O., and Mildren, R. P., “Thermal lens evolution and compensation in a high power KGW Raman laser,” Opt. Express 22(6), 6707-6718 (2014).
17. Geng, J., Sheng, Q., Fu, S., Shi, W., and Yao, J., “An efficient continuous-wave Nd:YVO_4/KGW intracavity Raman laser,” Opt. Lett. 48(24), 6364-6367 (2023).
18. Neto, J, Artlett, C., Lee, A., Lin, J. Spence, D., Piper, J., Wetter, N., and Pask H., “Investigation of blue emission from Raman-active crystals: Its origin and impact on laser performance,” Opt. Mater. Express 4(5), 889-902 (2014).
19. W. Koechner, *Solid-state laser engineering*, 6th ed., Springer Series in Optical Sciences (Springer, 2006).
20. Pask, H. M., “The design and operation of solid-state Raman lasers,” Prog. Quantum. Electron. 27(1), 3-56 (2003).
21. Mochalov, I. V., “Laser and nonlinear properties of the potassium gadolinium tungstate laser crystal $KGd(WO_4)_2$: Nd^{3+}-(KGW:Nd),” Opt. Eng. 36, 1660-1669 (1997).
22. Tu, Z., Guo, J., Gan, Z., Gao, Z., Gao, Y., Huang, Y., Guo, W., and Liang, X., “Dual-slab Yb:$KGd(WO_4)_2$ regenerative amplifier for spectral shaping and high-power output,” Opt. Lett. 48(23), 6263-6266 (2023).
23. Williams, R. J., Kitzler, O., Bai, Z., Sarang, S., Jasbeer, H., McKay, A., Antipov, S., Sabella, A., Lux, O., Spence, D. J., and Mildren, R. P., “High power diamond Raman lasers”, IEEE J Sel Top Quant. 24(5), 1602214 (2018).
24. Antipov, S., Sabella, A., Williams, R. J., Kitzler, O., Spence, D. J., and Mildren, R. P., “1.2 kW quasi-steady-state diamond Raman laser pumped by an M^2 = 15 beam”, Opt. Lett. 44(10), 2506-2509 (2019).

https://doi.org/10.1017/hpl.2024.5 Published online by Cambridge University Press